Supporting Information

Enhanced Surface Binding Energy Regulates Uniform Potassium Deposition for Stable Potassium Metal Anode

Xinxin Zhao,[a] Fengjiao Chen,[b] Junqing Liu,[c] Mingren Cheng,[a] Hai Su,[a] Jianbo Liu,[b] Yunhua Xu[a,d]*

[a]School of Materials Science and Engineering, Key Laboratory of Advanced Ceramics and Machining Technology (Ministry of Education), Tianjin Key Laboratory of Composite and Functional Materials, Tianjin University, Tianjin 300072, China.
E-mail: yunhua.xu@tju.edu.cn

[b]School of Materials Science and Engineering, Key Laboratory of Advanced Materials (MOE), Tsinghua University, Beijing 100084, China

[c]School of Materials Science and Engineering, National Institute for Advanced Materials, Nankai University, Tianjin 300350, China.

[d]Collaborative Innovation Center of Chemical Science and Engineering (Tianjin), Tianjin 300072, China.

Keywords: potassium metal anode, dendrite growth, SnO_2 coating layer, enhanced binding energy, 3D carbon fiber paper

Experimental Section

Preparation of PCNF mat

Porous carbon nanofiber (PCNF) mats were fabricated using electrospinning process and followed by high temperature carbonization. For electrospinning, the precursor solution was prepared by dissolving polyacrylonitrile (PAN, $M_W = 150{,}000\ g\ mol^{-1}$, J&K) into N,N-dimethylformamide (DMF, > 99.5%, Titan) and mechanically stirred at 80 °C overnight. Subsequently, electrospinning process was carried out by applying a voltage of 15 kV and a distance of 14 cm between the needle and the grounded roller. The flow rate of syringe pump was set to be 0.8 mL h^{-1}. The electrospun PAN mat was firstly stabilized at 280 °C for 3 h in air with a heating rate of 2 °C min^{-1} followed by high temperature carbonization at 800 °C for 2 h with a heating rate of 5 °C min^{-1} under nitrogen atmosphere.

Preparation of PCNF@SnO_2 and PCNF@SnO_2-K composite

The PCNF mat was attached onto the silicon wafer and transferred into a commercial ALD reactor with the exposure mode (MNT Micro and Nanotech Co., Ltd). ALD reactor chamber was heated to 175 °C and delivery lines were kept at 100 °C. Tetrakis(dimethylamino)tin (IV) (TDMASn, 99.999%, Strem) was kept at 50 °C and deionized water was kept at room temperature in stainless steel bottles. Nitrogen was used as the carrier gas and purge gas with a flow rate of 50 sccm. The ALD reactor was sustained at a low level of base pressure (typically 0.4 Torr) by a vacuum pump. The ALD-SnO_2 procedures were set as follows: (1) a 0.5 s supply of TDMASn; (2) a 10 s extended exposure of TDMASn to PCNF; (3) a 20s purge of excess TDMASn and any by-products; (4) a 1 s supply of H_2O; (5) a 10 s extended exposure of H_2O to PCNF; (6) a 20 s purge of excess H_2O and any by-products. Facile molten infusion was performed under ~250 °C (Movie S1) in an argon-filled glovebox (H_2O, $O_2 < 0.1$ ppm) to embed K into the 3D PCNF framework. Finally, the PCNF@SnO_2-K composite was obtained with an average weight of ~11 mg.

Theoretical calculation of binding energies between K atom with C and SnO_2

The first principle calculations were conducted in the framework of density functional theory (DFT) using Vienna ab initio simulation package.[S1] The projector augmented-wave approach was used to describe the interaction between the core and valence electrons.[S2] The kinetic energy cutoff was set to 520 eV. The geometries and the electronic structures were relaxed using the Perdew-Burke-Ernzerhof generalized-gradient approximation for the exchange-correlation functional.[S3] The *k*-point sampling employed a 1×1×1 mesh within the Γ–centered scheme. For the calculations of K adsorbed on the surface of the substrates, the van der Waals interaction was considered using a dispersion correction term with the DFT-D3 method.[S4] The convergence criteria for the energy and force were set to 10^{-5} eV and 0.02 eV $Å^{-1}$, respectively. For quantization the interaction between K atom and substrates, we defined the binding energy E_b as follows:

$$E_b = E(\mathrm{Sub}) + E(\mathrm{K}) \times N - E(\mathrm{Total})$$

E (Sub), E (K), and E (Total) represent the total energies of the substrate, the K atom, and the adsorption pair of the substrate and K atoms, respectively. N is the number of K atoms that are bound to the surface.

Materials and structural characterization

Morphology and structure of PCNF mat, PCNF@SnO_2 and PCNF@SnO_2-K composites were characterized on field-emission scanning electron microscopy (FESEM, Hitachi, S-4800), transmission electron microscopy (TEM, JEOL, JEM-2100F), X-ray diffraction (XRD, Rigaku Ultima IV, Cu Kα radiation source, λ = 1.5418 Å) and Raman spectra (Renishaw InVIA Reflex, 532 nm). SEM and TEM energy dispersive X-ray spectroscopy (EDS) were both performed on Oxford energy spectrometer. X-ray photoelectron spectroscopy (XPS) measurement was conducted on a Thermo Scientific K-Alpha X-ray photoelectron spectrometer with mono Al Kα radiation.

Electrochemical characterization

In all electrochemical measurements, CR2032-type coin cells were assembled in an argon-filled glove box (H_2O, $O_2 < 0.1$ ppm), using Celgard®2400 (Celgard, LLC Corp.) as separator and 50 μL 1.0 M potassium bis(fluoroslufonyl)imid (KFSI)-dimethoxyethane (DME) as electrolyte for each cell. And all batteries were tested on Neware BTS-5V10mA (Shenzhen) instrument at ambient temperature.

In symmetric cells, same electrodes (bare K or PCNF@SnO_2-K) were used as working and counter electrodes to evaluate the overpotentials. In order to evaluate the Coulombic efficiency, PCNF@SnO_2 composite electrodes were applied as working electrodes and bare K as counter electrodes. The cells were first run 5 cycles in a voltage window of 0-1.0 V at a current density of 0.5 mA cm^{-2} to remove any surface contamination and form a stable SEI layer. Galvanostatic plating of K was then carried out at the desired current density and areal capacity, followed by stripping of K by charging to a cutoff voltage of 0.5 V vs. K^+/K. The Coulombic efficiency for each cycle was calculated as the ratio of the capacity of K stripped to that of K deposited. All current densities were based on the area of the electrodes. Electrochemical impedance spectrometry (EIS) test was performed on a Solartron electrochemical workstation (1400+1470) in a frequency range of 0.01 Hz to 1 MHz with an ac amplitude of 5 mV.

Full cell fabrication

First, anthraquinone-1,5-disulfonic acid sodium salt (AQDS) powder and carbon black were ball-mixed at 300 rpm for 2 h with a weight ratio of 7: 2. Then the AQDS cathodes were prepared by casting slurry on the Al current collectors, which contains AQDS active material, carbon black and sodium alginate (SA) at a ratio of 7: 2: 1. The electrodes were dried at 80 °C overnight before cell assembly and the areal mass loading is 1.0-1.5 mg cm^{-2}. The applied current and capacity in the full cells are calculated based on the cathode weight.

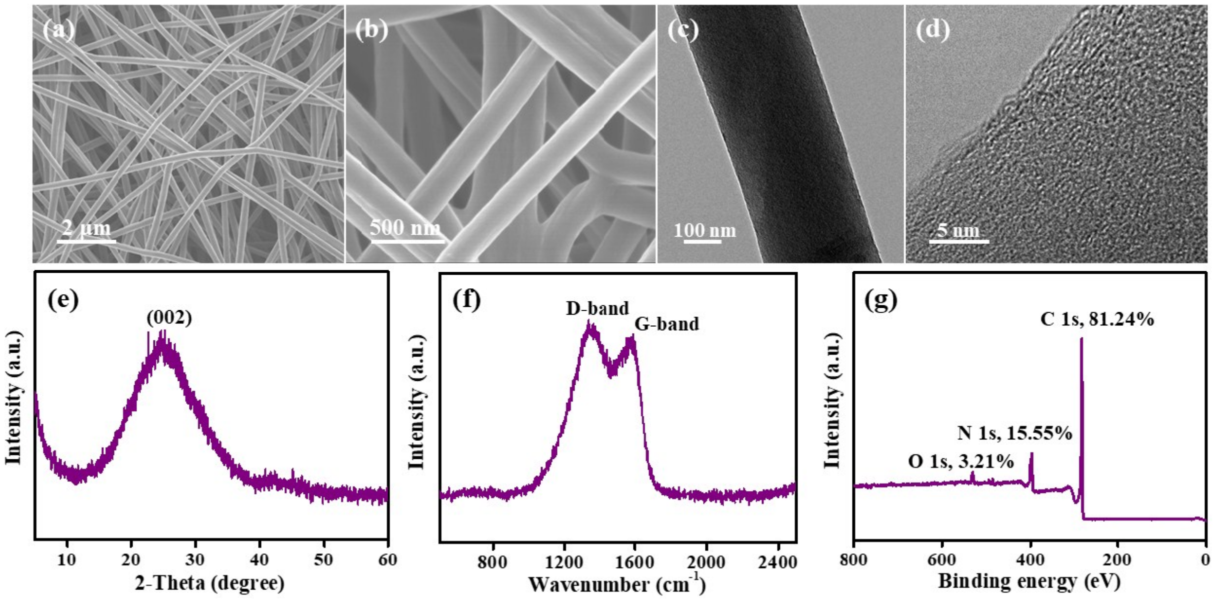

Figure S1. Morphology and structure characterization of PCNF mat: (a,b) SEM, (c) TEM and (d) HRTEM images, (e) XRD pattern, (f) Raman and (g) XPS survey spectra.

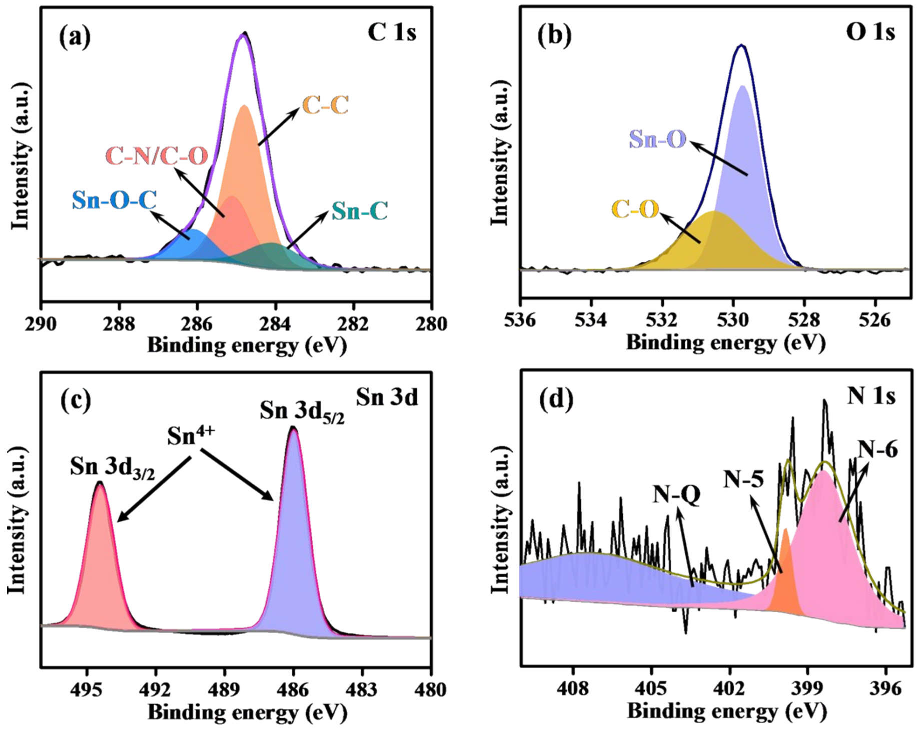

Figure S2. High resolution XPS spectra of PCNF@SnO_2 composite: (a) C 1s, (b) O 1s, (c) Sn 3d, and (d) N 1s.

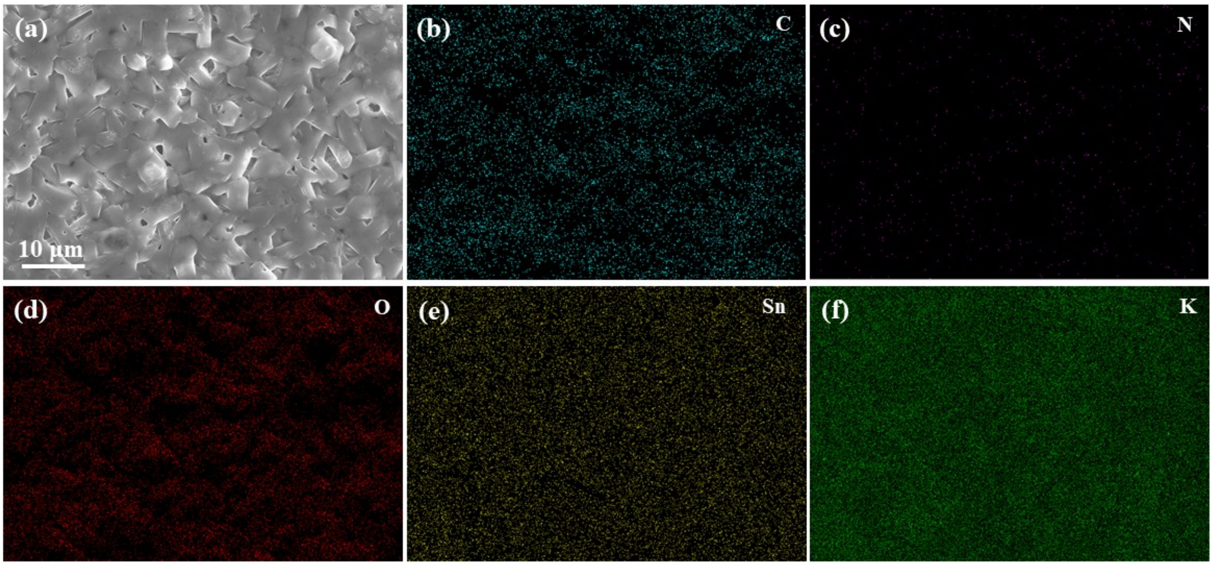

Figure S3. Morphology characterization of PCNF@SnO_2-K composite: (a) light field and (b-f) EDS element mapping images of C, N, O, Sn, K.

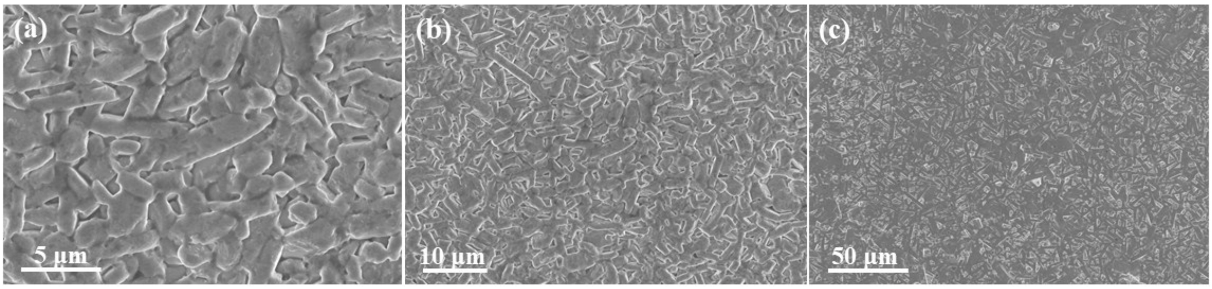

Figure S4. Morphology characterization of bare K electrode: (a-c) SEM images at different resolutions.

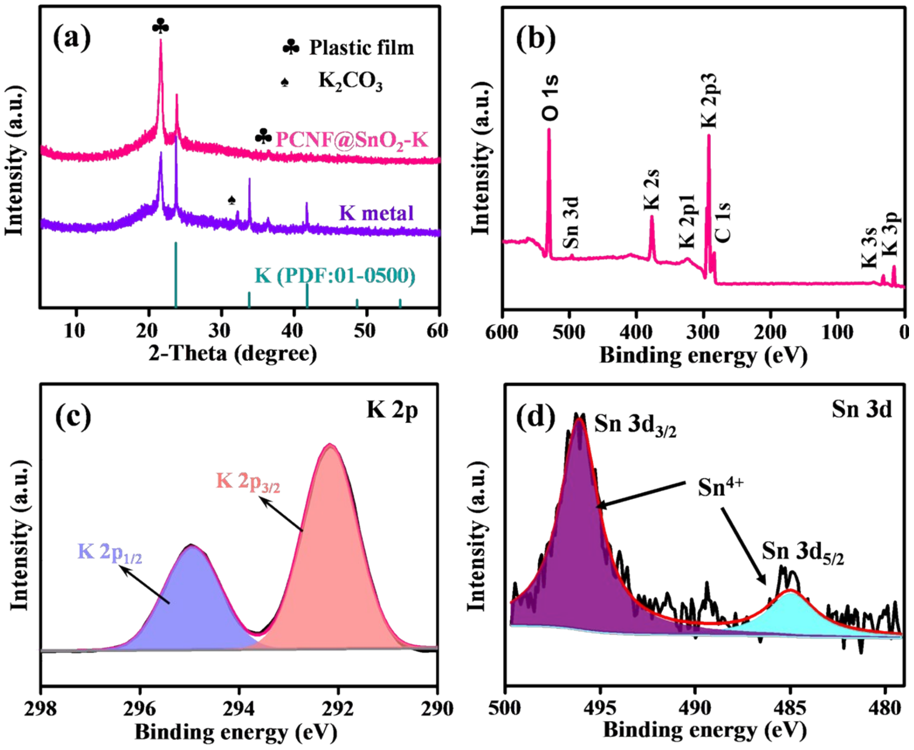

Figure S5. Chemical property analysis of PCNF@SnO$_2$-K composite: (a) XRD patterns of PCNF@SnO$_2$-K composite and bare K, (b) XPS survey and high resolution XPS profiles of (c) K 2p spectra, (d) Sn 3d spectra.

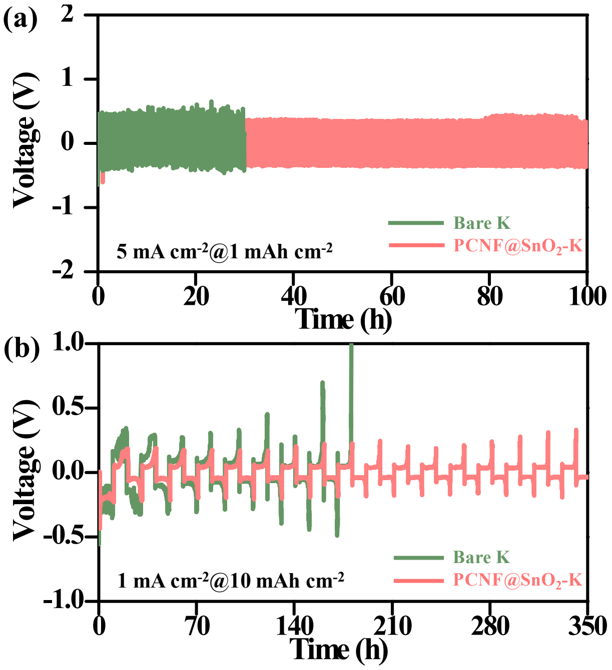

Figure S6. Galvanostatic cycling performance of PCNF@SnO$_2$-K composite and bare K anodes: (a) 5 mA cm^{-2}@1 mAh cm^{-2} and (b) 1 mA cm^{-2}@10 mAh cm^{-2}.

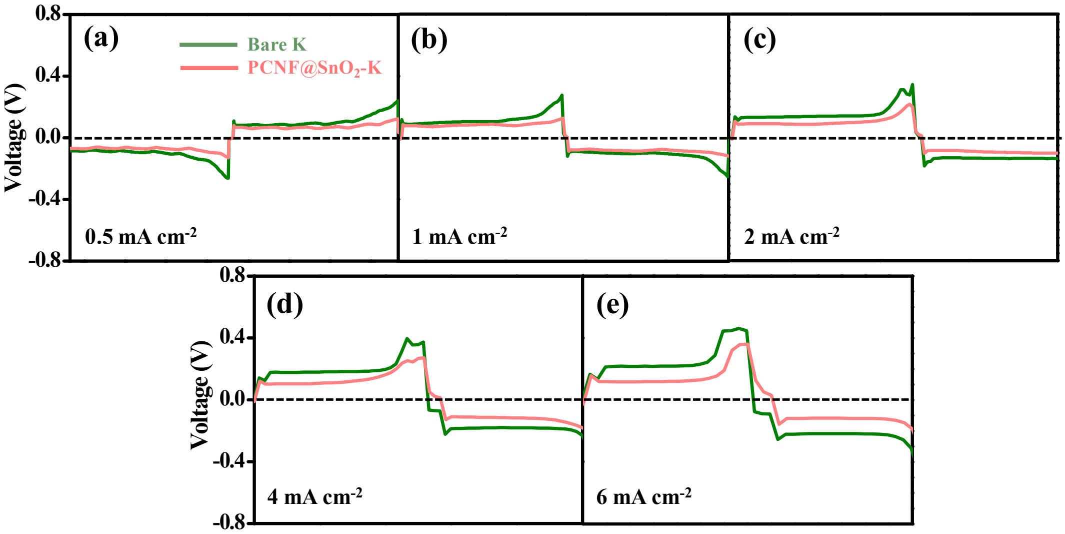

Figure S7. Specific voltage profiles of PCNF@SnO$_2$-K composite and bare K anodes at a capacity of 1 mAh cm^{-2} with different current densities (a) 0.5 mA cm^{-2}, (b) 1 mA cm^{-2}, (c) 2 mA cm^{-2}, (d) 4 mA cm^{-2} and (e) 6 mA cm^{-2}, respectively.

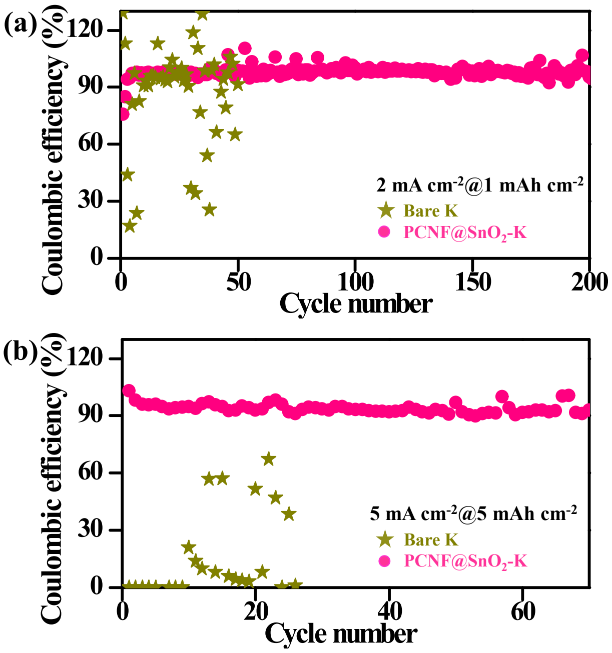

Figure S8. Coulombic efficiency of PCNF@SnO$_2$-K composite and bare K anodes at current densities and capacities of (a) 2 mA cm^{-2}@1 mAh cm^{-2} and (b) 5 mA cm^{-2}@5 mAh cm^{-2}.

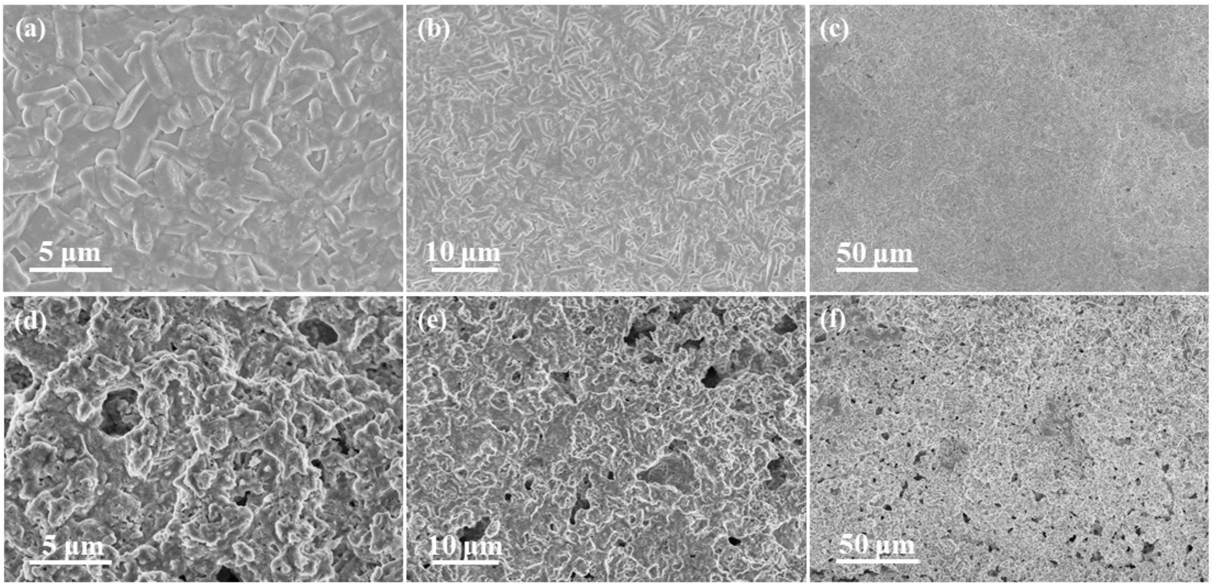

Figure S9. SEM images of (a-c) PCNF@SnO_2-K composite and (d-f) bare K anodes after 20 cycles at 1 mA cm^{-2}@1 mAh cm^{-2}.

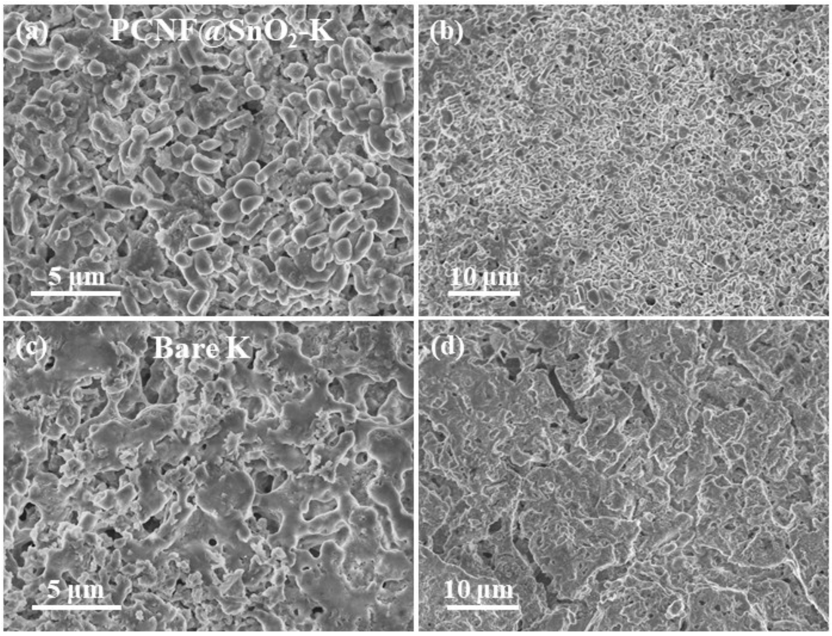

Figure S10. SEM images of (a,b) PCNF@SnO_2-K composite and (c,d) bare K anodes after 200 cycles at 1 mA cm^{-2}@1 mAh cm^{-2}.

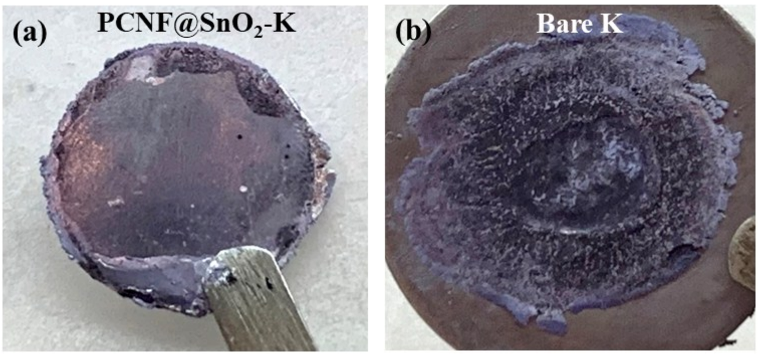

Figure S11. Optical photographs of (a) PCNF@SnO$_2$-K composite and (b) bare K anode taken from symmetric cells after 200 cycles at 1 mA cm^{-2}@1 mAh cm^{-2}.

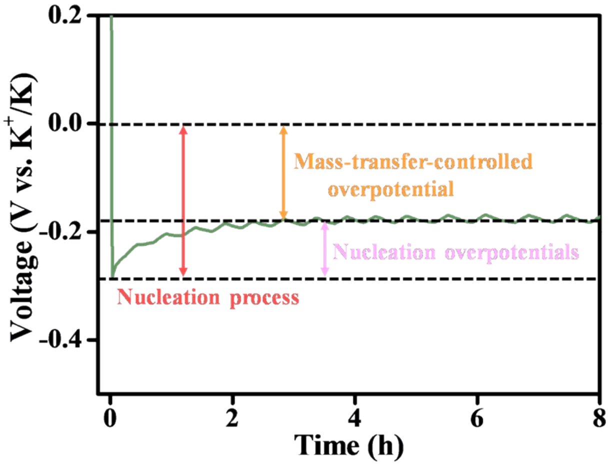

Figure S12. K nucleation behavior on PCNF@SnO$_2$ composite mat at 0.5 mA cm^{-2}.

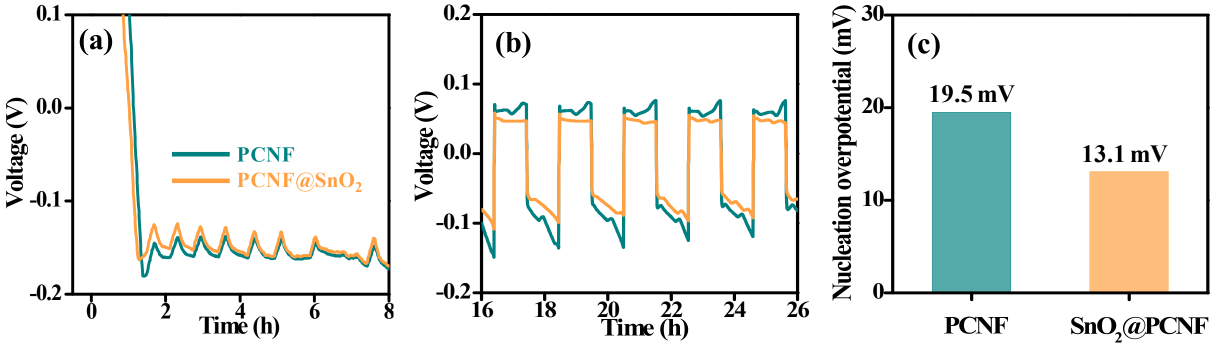

Figure S13. K plating/stripping behavior of PCNF and PCNF@SnO$_2$ composite mats: (a) K nucleation behavior at 0.5 mA cm^{-2}, (b) cycling performance at 1 mA cm^{-2}@1 mAh cm^{-2}, and (c) K nucleation overpotentials.

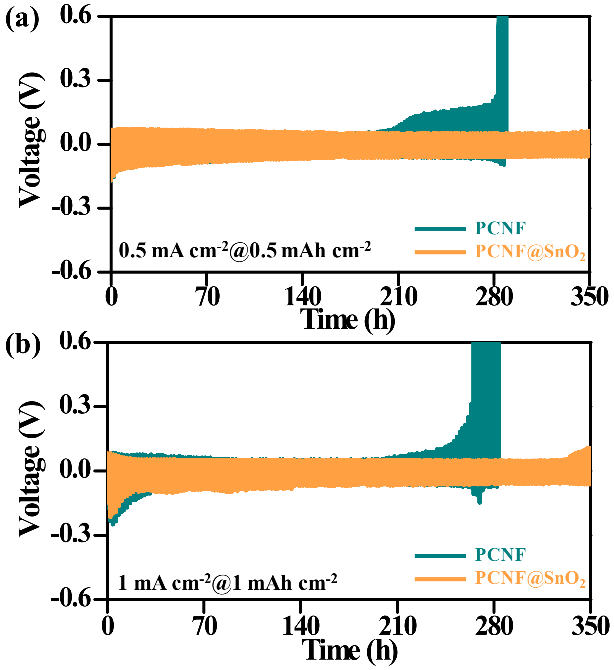

Figure S14. Galvanostatic cycling performance of PCNF@SnO_2 composite and PCNF mats with bare K as counter electrodes at (a) 0.5 mA cm^{-2}@0.5 mAh cm^{-2} and (b) 1mA cm^{-2}@1 mAh cm^{-2}. 4 mAh cm^{-2} K was pre-plated at 0.5 mA cm^{-2}.

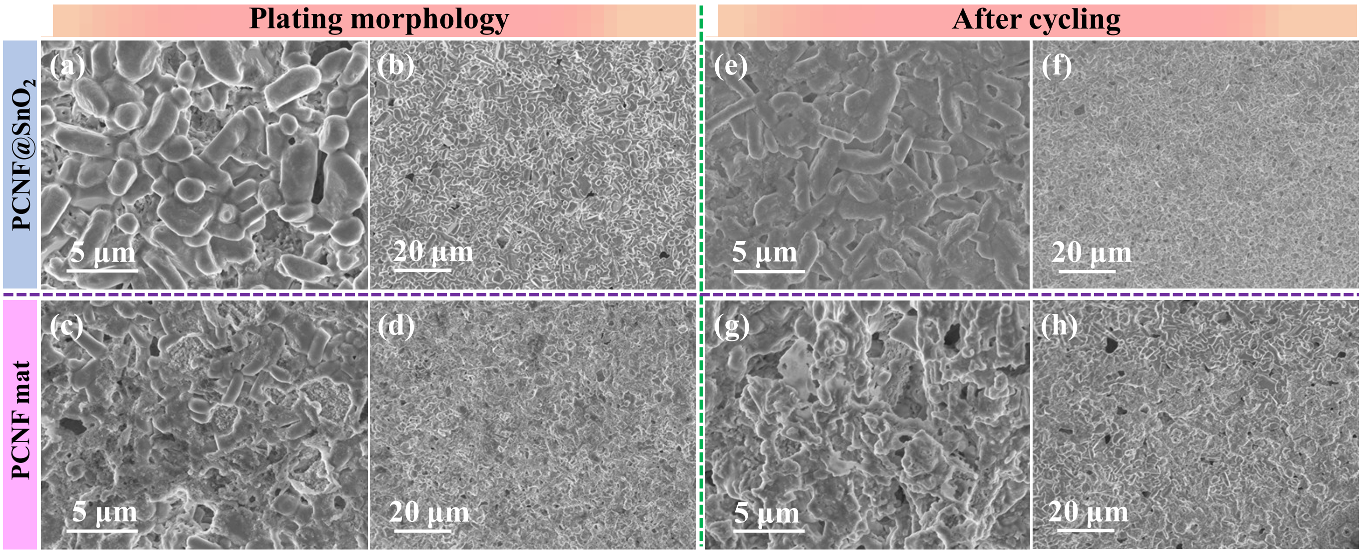

Figure S15. SEM images of (a,b,e,f) PCNF@SnO_2 composite and (c,d,g,h) PCNF mat of (a-d) upon K plating at 0.5 mA cm^{-2}@4 mAh cm^{-2} and (e-h) after 200 cycles at 1 mA cm^{-2}@1 mAh cm^{-2}.

Table S1. Comparison of electrochemical performance of K metal anodes.

Materials	Current density (mA cm^{-2})	Capacity (mAh cm^{-2})	Overpotential (mV)	Cycle life (h)	Ref.
PCNF@SnO$_2$-K	**1**	**1**	**46**	**1700**	**This work**
K-aligned Carbon nanotube membrane (ACM)	1	1	~100	230	S5
Puffed millet/NiO/K	0.4	0.4	~100	100	S6
K@DN-MXene/CNT	0.5		~300	300	S7
SnTFSI@3D-K	1	1	29	100	S8
Bare K (KFSI/DME)	0.05	---	~500	---	S9
Bare K (KFSI/EC+DEC)	1	1	300	200	S10
Bare K (KFSA/DME)	0.025	---	25	~320	S11
Carbon paper@Na-K alloy	0.4	0.8	~200	2800	S12
Carbon fiber cloth/K$_2$O layer@Na-K alloy	0.4	0.2	220	140	S13
CM@Na-K alloy	1	2	100	1600	S14
Carbon cloth@Na-K alloy	0.8	---	~185	---	S15

Table S2. Fitted EIS results of the symmetric cells using different metal anodes.

	R_{ct} (Ω)	**R_s (Ω)**
PCNF@SnO$_2$-K anode	4682	6.056
Bare K anode	11146	15.93

References

S1 G. Kresse and J. Furthmüller, *Phys. Rev. B*, 1996, **54**, 11169-11186.

S2 P. E. Blöchl, *Phys. Rev. B*, 1994*,* **50***,* 17953-17979.

S3 J. P. Perdew, K. Burke and M. Ernzerhof, *Phys. Rev. Lett.*, 1996, **77**, 3865-3868.

S4 S. Grimme, J. Antony, S. Ehrlich, H. Krieg, *J. Chem. Phys.*, 2010, **132**, 154104.

S5 L. Qin, Y. Lei, H. W. Wang, J. H. Dong, Y. Y. Wu, D. Y. Zhai, F. Y. Kang, Y. Tao and Q.-H. Yang, *Adv. Energy Mater.*, 2019, **9**, 1901427.

S6 Y. Q. Lia, L. Y. Zhang, S. F. Liu, X. L. Wang, D. Xie, X. H. Xia, C. D. Gu and J. P. Tu, *Nano Energy*, 2019, **62**, 367-375.

S7 X. Tang, D. Zhou, P. Li, X. Guo, B. Sun, H. Liu, K. Yan, Y. Gogotsi and G. X. Wang, *Adv. Mater.*, 2019, 1906739.

S8 M. H. Ye, J.-Y. Hwang and Y.-K. Sun, *ACS Nano*, 2019, **13**, 9306-9314.

S9 N. Xiao, W. D. McCulloch and Y. Y. Wu, *J. Am. Chem. Soc.*, 2017, **139**, 9475-9478.

S10 H. Wang, D. D. Yu, X. Wang, Z. Q. Niu, M. X. Chen, L. W. Cheng, W. Zhou and L. Guo, *Angew. Chem. Int. Ed.*, 2019, **58**, 16451-16455.

S11 T. Hosaka, S. Muratsubaki, K. Kubota, H. Onuma and S. Komaba, *J. Phys. Chem. Lett.*, 2019, **10**, 3296-3300.

S12 L. G. Xue, H. C. Gao, W. D. Zhou, S. Xin, K. Park, Y. T. Li, J. B. Goodenough, *Adv. Mater.*, **2016**, *28*, 9608-9612.

S13 L. Y. Zhang, X. H. Xia, Y. Zhong, D. Xie, S. F. Liu, X. L. Wang and J. P. Tu, *Adv. Mater.*, 2018, **30**, 1804011.

S14 L. Qin, W. Yang, W. Lv, L. Liu, Y. Lei, W. Yu, F. Y. Kang, J.-K. Kim, D. Y. Zhai and Q.-H. Yang, *Chem. Commun.*, 2018, **54**, 8032-8035.

S15 Y. Ding, X. L. Guo, Y. M. Qian, L. Y. Zhang, L. G. Xue, J. B. Goodenough and G. H. Yu, *Adv. Mater.*, 2019, **31**, 1806956.